Novel Castor Oil/Water/Ethanol Pickering Emulsions Stabilized by Magnetic Nanoparticles and Magnetically Controllable Demulsification

Mohammad Jahid Hasan,[a] Peng Chen,[b] Neithan Dominick,[a] Erick S. Vasquez,[b,c] Esteban Ureña-Benavides[a,*]

[a] *Department of Biomedical Engineering and Chemical Engineering, The University of Texas at San Antonio, One UTSA Circle, San Antonio, 78249, TX, USA*

[b] *Department of Chemical and Materials Engineering, University of Dayton, 300 College Park, Dayton, OH, 45469-0256, USA*

[c] *Integrative Science and Engineering Center, University of Dayton, 300 College Park, Dayton, OH, 45469, USA*

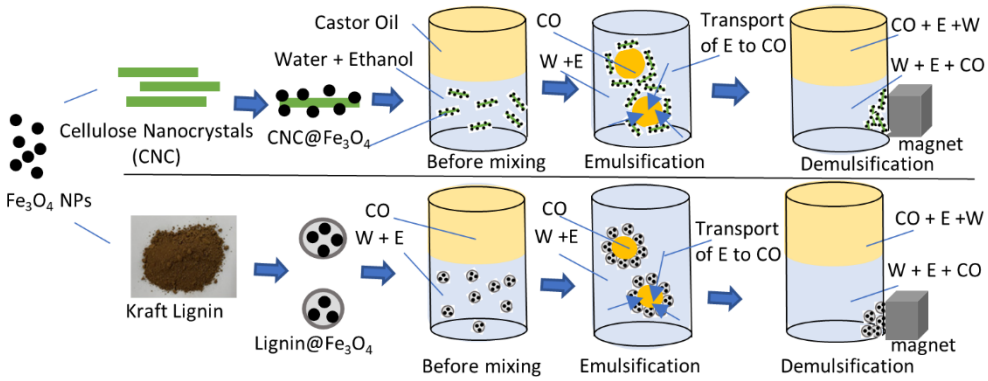

Three-component castor oil/water/ethanol Pickering emulsions were prepared by mixing castor oil and ethanol-water solution stabilizing by CNC@Fe_3O_4 and Lignin@Fe_3O_4 magnetic nanoparticles and magnetically demulsified by using a permanent magnet.

ABSTRACT

A novel castor oil/water/ethanol Pickering emulsion, stabilized by magnetic nanoparticles (NPs), was developed to allow on-demand demulsification by an external magnetic field for the extraction of ethanol from aqueous solution using the castor oil. The emulsion was stabilized by Fe_3O_4-coated cellulose nanocrystals (CNC@Fe_3O_4) and lignin-coated Fe_3O_4 NPs (lignin@Fe_3O_4). The stability of the emulsions was investigated at various castor oil to ethanol-water ratios (50/50 and 70/30), various NP concentrations, and ethanol concentrations in the aqueous phase. The magnetically controlled demulsification ability of the emulsions was investigated by using a permanent magnet. The results showed that the 70/30 emulsions were more stable than the 50/50 emulsions for all the ethanol concentrations. Moreover, increasing the NP concentration increased the emulsion stability and hence, 1 w/v% NPs concentration provided the more stable systems. However, all the emulsions were successfully broken by the permanent magnet. Yet, the presence of ethanol improves the ability of the external magnetic field to demulsify these dispersions. Furthermore, the used hybrid NPs were recovered and recycled for three cycles. The recycled NPs were characterized with X-ray diffraction (XRD) and vibrating sample magnetometry (VSM) indicating that they retained their saturation magnetization and crystalline structure, demonstrating their lack of degradation over multiple recycling cycles. This study facilitates

the exploration of innovative two-phase Pickering emulsions comprising three distinct liquid components and their utilization in liquid-liquid extraction processes.

KEYWORDS: Pickering emulsion, Demulsification, Iron oxide nanoparticles (IONPs), Castor oil water ethanol, Magnetic separation, Extraction of ethanol

1. Introduction

The biological synthesis of ethanol has been extensively studied as a sustainable route to biofuel production. However, separating ethanol from the aqueous fermentation mixture is often achieved through an energy intensive distillation, followed by water adsorption with molecular sieves. Liquid/liquid extraction followed by flash separation is a promising alternative route to achieve this separation with a lower cost and energy consumption. In fact, Offeman et al. (2006) proposed the use of castor oil, as a renewable, low volatility and non-toxic solvent to achieve this separation, and compared it to other vegetable oils and extraction solvents [1]. However, these systems often form relatively stable emulsions that need to be broken to complete the separation, as such industrial liquid/liquid extraction equipment have large settler regions with coalescence plates needed to obtain decantable immiscible liquid phases; thus, there is a practical need to increase the rate of demulsification of these systems in a controllable manner. This paper focuses on the stability of Pickering emulsions stabilized with nanocomposite magnetic nanoparticles and the accelerated demulsification by an external magnetic field, as relevant to the extraction of ethanol from aqueous solutions.

Pickering emulsions are stabilized by adsorbed solid particles rather than emulsifiers [2–8]. An additional advantage of Pickering emulsions over traditional emulsions stabilized by emulsifiers is their improved stability [9,10]. Solid particle covering of droplets creates a formidable barrier against coalescence, stabilizing concentrated emulsions efficiently. Adsorbed solid particles are stabilized in the oil-water interface by being partially wetted by both immiscible liquid phases. In addition, magnetic nanoparticles (NPs) have been utilized to stabilize Pickering emulsions for a wide range of applications, including magnetically controllable emulsification and demulsification, oil recovery, wastewater treatment, magnetic separation, and liquid-liquid extraction [11–18].

Iron and iron oxide-based NPs are among the most common types of magnetic NPs utilized to stabilize Pickering emulsions [19–22]. Pavia-Sanders et al. reported that polyvinylpyrrolidone-coated Fe_3O_4 NPs had an exceptional capacity to remove oil in a short period of time (40 min) [23]. Similarly, Fe_3O_4/PS nanocomposites and superparamagnetic Fe_3O_4/β-cyclodextrin have been shown to remove oil from water [24]. Bare Fe_3O_4 NPs are hydrophilic and can be used to stabilize o/w emulsions [19]; however, the surface of the Fe_3O_4 NPs can be adjusted to become hydrophobic depending on the coating materials used for stabilizing the particles.

Cellulose and lignin are two of the most abundant natural biopolymers on earth. Cellulose and lignin-based NPs have been investigated for many decades because they are low-cost, non-toxic, renewable, and biocompatible [25–27]. Both cellulose nanocrystals and lignin nanoparticles are amphiphilic [28,29] and they have been employed in Pickering emulsions by various authors [4,10,30–33]. Moreover, binding iron oxide nanoparticles to cellulose or lignin NPs make the hybrid nanoparticles suitable for magnetically controllable Pickering emulsions and magnetically induced oil-water separations [11,13,22,34–36]. Recently, our group developed castor oil/water Pickering emulsions by utilizing CNC@Fe_3O_4 NPs [13]. Mikhaylov et al. developed magnetite/cellulose nanocrystal-stabilized liquid paraffin oil-in-water Pickering emulsions and investigated the adsorption of chromium ions on the emulsions [22]. Low et al. synthesized Fe_3O_4-cellulose nanocrystals (MCNC) via ultrasound assisted co-precipitation method to stabilize palm olein-in-water Pickering emulsion [35]. Later, Low et al. reported using Fe_3O_4@cellulose nanocrystals-stabilized Pickering emulsions containing curcumin to magnetically trigger drug

release [34]. On the other hand, the synthesis and applications of multifunctional magnetic-lignin nanoparticles in Pickering emulsions are less studied. Recently, Hasan et al. utilized lignin@Fe_3O_4 nanoparticles in magnetically controllable castor oil/water Pickering emulsion and oil herding [11]. Although, there are few examples of magnetic nanoparticles and lignin-based hybrid materials being used in Pickering emulsions and separation processes [37–40].

Demulsification is the process of separating an emulsion into its component phases, often by separating the dispersed droplets from the continuous phase. Magnetic NPs have been used in stabilizing Pickering emulsions and demulsified on-demand with various types of magnetic fields in literature [11,13–15]. In our previous studies, we successfully demulsified castor oil-water Pickering emulsions, stabilized by CNC@Fe_3O_4 NPs and lignin@ Fe_3O_4 NPs, using a permanent magnet, although in the case of CNC@Fe_3O_4, only the water/oil emulsions could be broken, while the oil/water emulsions remained emulsified after 24 h on a permanent magnet [11,13]. Previously, Yang et al. (2020) successfully studied demulsification of carbonyl iron particle (CIP) stabilized Pickering emulsions by using alternating magnetic field [15]. In another study, water-in-oil (W/O) type commercially-available crude oil emulsion was successfully demulsified by using a permanent magnet and an electromagnetic field [16].

A number of parameters influence emulsion stability, including emulsifier type and concentration, droplet size and dispersion, processing conditions, electrolyte concentration, etc. [9,10]. Hydrophilic particles are known to promote the formation of oil-in-water (o/w) emulsions, whereas hydrophobic particles typically tend to enable water-in-oil (w/o) emulsions [41]. However, amphiphilic particles with both hydrophilic and hydrophobic groups on their surface are known to produce either o/w or w/o emulsions depending on the interaction between the particles and the oil-water interface [42,43].

In this paper, various castor oil/ethanol/water emulsions were stabilized by CNC@Fe_3O_4 NPs and lignin@ Fe_3O_4 NPs and were then broken on-demand by using a permanent magnet. Although, there are other examples of research articles that reported Pickering emulsions' stability and magnetically controlled demulsification, most of the research was conducted for conventional two-component Pickering emulsions [2-8]. Here, we concentrated our efforts on conducting a comprehensive investigation into the stability of two-phase Pickering emulsions involving three components relevant to the liquid/liquid extraction of ethanol from water. It investigates a variety of factors affecting the stability of the castor oil/water/ethanol emulsions such as NP concentrations, oil to water ratios, ethanol concentrations, NP film wettability, and interfacial tension of the ternary system at equilibrium conditions. Additionally, we explored the application of magnetically controlled demulsification in the presence of ethanol, and the recyclability of the nanoparticles. Notably, this paper investigated the change in magnetic properties of the nanoparticles after three cycles of emulsification/demulsification/decantation steps to demonstrate their limited degradation after recycling.

2. Experimental section

2.1. Materials

Iron (III) chloride hexahydrate (>97% purity), iron (II) chloride tetrahydrate (>96% purity), Sulfuric acid (>96% purity), ammonium hydroxide (28.0 to 30.0 w/w %), Sudan Red (> 90% purity), and amaranth (>85% purity) were all bought from Thermo Fisher Scientific (Waltham, MA) and were used as received. Castor oil (>99.5% purity) and Kraft lignin (95% Purity) were purchased from Sigma Aldrich (St. Louis, MO) and used as received. Southern bleached softwood Kraft pulp cellulose was kindly gifted by Weyerhaeuser pulp mill (Columbus, MS).

2.2. Synthesis of CNC, bare Fe_3O_4, CNC@Fe_3O_4 and lignin@Fe_3O_4

Cellulose nanocrystals (CNCs) were isolated first from the SBSK wood pulp using the procedure described in our previous publication [25]. In short, the cellulosic wood pulp was hydrolyzed using sulfuric

acid at 45 °C for 50 minutes with stirring. After completion, the reaction mixture was diluted with cold deionized water and purified by removing the excess acid. CNC@Fe_3O_4 NPs were synthesized by the deposition of Fe_3O_4 NPs onto CNCs at a mass ratio of 1:4 (CNC: Fe_3O_4) through a one-step coprecipitation using iron chloride salts and NH_4OH in a N_2 atmosphere at 90 °C. Upon completion the reaction was cooled and the NPs separated using a Neodymium permanent magnet and washed with DI water. A detailed description of the synthesis of all the NPs is provided in the Supplementary Material (SM), section 1.1.

Bare Fe_3O_4 were synthesized according to our previous publications as described in the SM, section 1.2 [11,31]. The liginin@Fe_3O_4, was then prepared by coating the bare Fe_3O_4 NPs with lignin according to our previous publication [11]. The Kraft lignin (KL) was first dissolved in a 1 wt% sodium hydroxide solution. Then, this alkaline KL solution was sonicated and pumped into 1-L vessel containing the bare Fe_3O_4 NPs at a rate of 15 mL/min. The final ratio of KL to Fe_3O_4 was 3 to 1. The vessel contents were mixed for 25 minutes at 600 RPM to synthesize lignin@Fe_3O_4 NPs. Upon completion of the reaction, the NP were purified by a magnetic separation and subsequent washes with DI water. Then they were dried in a lyophilizer and ground into a fine powder using a mortar and pestle. A more detailed description is provided in SM, section 1.3.

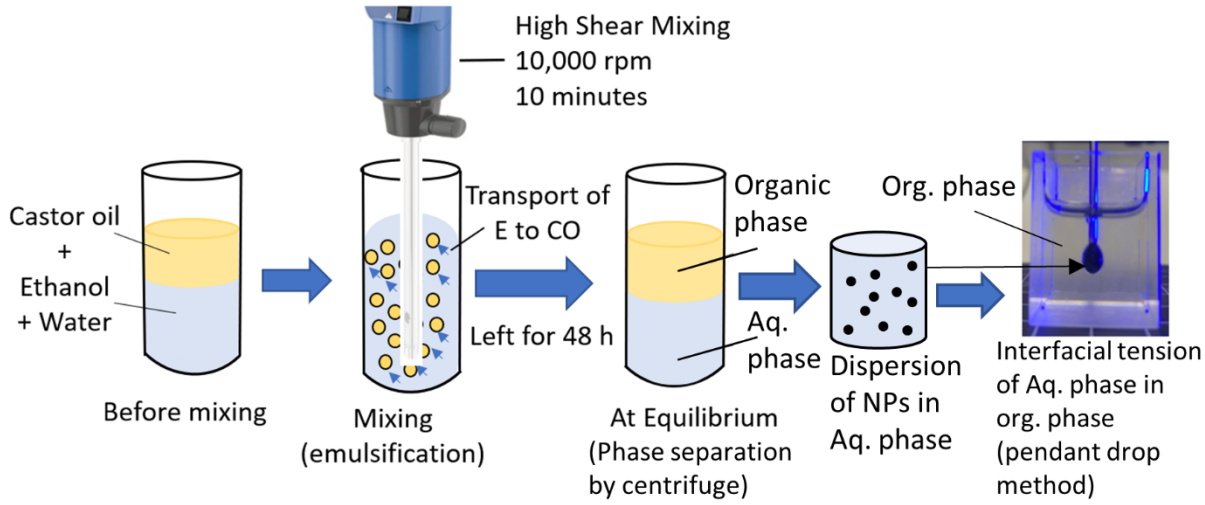

Figure 1. Pendant drop method used to measure the interfacial tension between aqueous and organic phases in equilibrium with each other for the ternary mixture of castor oil, water, and ethanol in the presence of nanoparticles.

2.3. Characterizations of CNC, bare Fe_3O_4, CNC@Fe_3O_4 and lignin@Fe_3O_4 and recycled NPs

A JEOL (Peabody, MA) JEM-2010 F TEM was utilized to collect Transmission Electron Microscopy (TEM) pictures. To prepare the samples, approximately 5 microliters of a dilute solution were deposited onto a copper carbon mesh grid (CF300-Cu grids, Electron Microscopy Science) and permitted to dry within a well-ventilated hood for a minimum of 24 hours before collecting the pictures.

TGA data was gathered using a TGA Q500 (TA Instruments, New Castle, DE) to investigate the thermal stability of the NPs, as well as the amount of Fe_3O_4 in the hybrid NPs. A balancing nitrogen flow of 10 mL/min and a sample nitrogen flow rate of 90 mL/min was employed for all samples, coupled with a temperature range from 25 – 800 ºC with a constant ramp rate of 10 ºC/min. At least 5 mg of material was put on a platinum pan to achieve reliable findings. The amount of lignin and CNC content in the lignin@Fe_3O_4 and CNC@Fe_3O_4 NPs was calculated based on methods described in our previous publications [11,13], and shown in the supporting information.

Magnetization measurements of the NPs were collected using a vibrating sample magnetometer (Quantum Design Versalab, San Diego, CA) at room temperature (300 K). The normalized moment (emu/g) for each sample as a function of magnetic field was reported based on the weight of each NP sample.

Powder X-ray diffractograms (XRD) were collected using Malvern Panalytical Empyrean Nano Edition (Westborough, MA). The NPs dispersions were freeze-dried and scanned from 2θ = 10° to 80° at a step time of 0.6 s/step (0.003°/step) and sample revolution of 4 rev/min at 25 °C with Cu Kα radiation (λ = 0.1540nm).

The zeta potential and Z-average hydrodynamic diameter of the nanoparticles (NPs) were measured using a Malvern Zetasizer Nano ZS (Malvern Instruments, United Kingdom). To conduct the measurements, a diluted solution with a low concentration (0.1 wt%) of each sample was prepared, and the assessments were carried out under pH 7 conditions.

2.4. Determination of wettability of the nanoparticles

The wettability of the nanoparticles was determined by measuring the water contact angle of the various thin films prepared by the nanoparticles. Contact angle measurements were performed following the sessile drop method with a Kruss drop shape analyzer (model: DSA 100 S, Kruss Scientific, Hamburg, Germany). In short, a liquid suspension containing 1 wt % NPs was prepared first, then, 100 µl of the suspension was put on a clean substrate (micadisc, diameter 10 mm, Tedpella Inc., Redding, CA) followed by drying of the liquid overnight in a vacuum oven. Hence, a thin film was prepared and then the static water contact angle was measured by placing a 29 µl droplet of water (using a 1 ml-size syringe and 1.825 mm outer diameter size needle) on the thin film and measuring the angle formed between the droplet and the surface.

2.5. Determination of interfacial tension of the nanoparticles at the castor oil-water-ethanol interface

The interfacial tension of castor oil, water and ethanol was measured at equilibrium conditions in the presence of NPs. Briefly, 7 ml castor oil, 2.7 ml water and 0.3 ml ethanol were mixed with a high shear mixer (IKA Ultra-Turrax T-25 Basic, Atkinson, NH) at 10000 rpm for 10 minutes. Then the mixture was allowed to rest for 48 h to reach thermodynamic equilibrium [12]. After 48 hours, the mixture was centrifuged using a benchtop centrifuge (model 5804 R, Eppendorf, Hamburg, Germany) at 11000 rpm (RCF 16639 × g, Eppendorf Rotor FA-45-6-30) to complete the phase separation. Once the organic phase and the aqueous phases were separated, they were taken out. Then dry CNC@Fe_3O_4 and lignin@Fe_3O_4 were dispersed in the aqueous phase at various concentrations (0, 0.25, 0.5, 0.75, and 1 w/v%). The organic phase was taken into a transparent cuvette and a droplet of aqueous NPs suspension was created by using a 1 ml size syringe and 1.825 mm outer diameter size needle and placed inside the organic phase (Fig.1). Each droplet (~ 90 µL) was equilibrated in the organic phase for 1 hour. The interfacial tension was determined using a Kruss drop shape analyzer (model: DSA 100 S, Kruss Scientific, Hamburg, Germany) by droplet shape analysis and the Young Laplace equation. The dynamic interfacial tension was collected for 1 hour, and the value of interfacial tension after 1 hour was reported as the equilibrium interfacial tension.

2.6. Preparation of castor-oil/water/ethanol Pickering emulsions

Pickering emulsions of the three-component system were prepared by mixing the castor oil and ethanol with the CNC@Fe_3O_4 or lignin@Fe_3O_4 NPs' colloidal aqueous suspensions. Stock dispersions of 4 wt% CNC@Fe_3O_4 and 4 wt% lignin@Fe_3O_4 were prepared first. To prepare the emulsion of 10 ml each, the required amount of CNC@Fe_3O_4 or lignin@Fe_3O_4 stock suspension was added to a vial first, followed by the addition of water (if needed), ethanol, and castor oil, in that order. The relative amounts of each component were adjusted to give final NP concentrations of 0, 0.25, 0.5, 0.75, or 1.0 w/v%, ethanol concentrations in the initial aqueous phase of 0%, 5%, 10%, 15%, and 20 vol% and castor oil aqueous phase volume ratio of 50/50 or 70/30. The samples were then mixed thoroughly with a high shear mixer (IKA Ultra-Turrax T-25 Basic, Atkinson, NH) at 10000 rpm for 2 minutes. Once the emulsions were prepared, pictures of the vials were taken at 0 h, 1 h, and 24 h, and 48 h with a digital camera to monitor emulsion creaming.

Microscopic pictures of the emulsions were also taken using an optical microscope (AmScope 500MD) and a 13 mm ID x 0.12 mm deep spacer. The droplet size distributions were determined by measuring at least 300 droplets with Image J. Similar to Qiao et al., the drop test technique was utilized to identify the kind of emulsions [44] and determining the dispersion phase and continuous phase using the dye amaranth.

2.7. Magnetically controllable demulsification

Demulsification of the Pickering emulsions prepared with castor oil, water, ethanol and stabilized by CNC@Fe_3O_4 or lignin@Fe_3O_4 was investigated with an external magnetic field. In brief, the emulsion vials were placed beside a neodymium N42 grade magnet (size 2×2×1 inch, Applied Magnets, AOM05648221). The effect of the magnetic field on demulsifying the emulsions was examined by photographing the vials at 0 h, 1 h, and 24 h using a digital camera. An optical microscope (AmScope 500MD) was also used to capture microscopic images of the emulsion droplets, and droplet size distributions were estimated by analyzing at least 300 droplets with image J.

2.8. Recycling of CNC@Fe_3O_4 and lignin@Fe_3O_4

The CNC@Fe_3O_4 and lignin@Fe_3O_4 nanoparticles were recovered after demulsification. After demulsification, the separated organic and aqueous phases were taken out from the vial. A permanent magnet was kept beside the vial to avoid the loss of magnetic nanoparticles while decanting both liquid phases. Then the magnetic nanoparticles were washed with ethanol first, followed by a wash with water twice. The recovered NPs were dried in a freeze drier (Labconco, Freezone, 6 L Benchtop 115) and then redispersed in DI water by probe sonication for 1 minute (Amplitude: 30; 1 s on and 1 s off). The aqueous magnetic NP suspension was then reused in the following magnetically controllable emulsification/demulsification cycle. This process was repeated twice more to complete three cycles.

2.9. Statistical Analysis

Statistical Analysis was performed to verify changes in means of droplet sizes at 95% confidence [4,45]. The emulsion droplets were log-normally distributed, and z statistics test was carried out to compare the droplet sizes at varying nanoparticles concentrations as well as changes of droplet sizes over time. A detail of the statistical method used in this study is provided in the Supplementary Material Section 4. The test results of the various hypothesis tests are also provided in the Supplementary Material (Table S1).

3. Results and discussion

3.1. *Characterizations of CNC@Fe_3O_4 and lignin@Fe_3O nanoparticles*

CNC@Fe_3O_4 and lignin@Fe_3O_4 NPs were characterized through a variety of experimental methods. Fig 2A shows the TEM image of CNC@Fe_3O_4 NPs and it demonstrates that the CNCs were completely coated with Fe_3O_4 NPs, however, with some aggregation. These aggregates are expected to be useful in stabilizing Pickering emulsions [13]. On the other hand, the TEM image of lignin@Fe_3O_4 NPs (Fig 2B) shows that the Fe_3O_4 NPs clusters were coated with lignin. Hence, CNC@Fe_3O_4 nanocomposites have the Fe_3O_4 NPs on their surface whereas lignin@Fe_3O_4 NPs contain the Fe_3O_4 in the core with a lignin shell. Thus, the surface properties of the CNC@Fe_3O_4 and lignin@Fe_3O_4 NPs varied and they were further characterized with various instrumental techniques. A summary of the results is presented in Table 1.

Table 1. Characterization of CNC@Fe_3O_4 and lignin@Fe_3O_4 NPs

Characterization	Method used	CNC@Fe_3O_4	lignin@Fe_3O_4	Bare Fe_3O_4
Zeta potential at pH 7	Zetasizer	-33 ± 1 mV	-40 ± 1 mV	-20 ± 2 mV
Hydrodynamic diameter in water (at pH 7) at 0 h	DLS	221 ± 5 nm	161 ± 4 nm	33 ± 7 nm
Hydrodynamic diameter in water after 2 h	DLS	321 ± 10 nm	274 ± 9 nm	1645 ± 45 nm
Fe_3O_4 content in the sample	TGA	74.1 ± 5.1 wt%	78.6 ± 2.1 wt%	~ 100 wt%
Saturation magnetization	VSM	62 ± 1 emu/g	58 ± 1 emu/g	77 ± 1 emu/g
Water contact angle	Sessile drop	44° ± 3°	50° ± 2°	25° ± 5°

The magnetite content in the nanocomposites was determined by thermogravimetric analysis. A detailed procedure for the calculation of magnetite content is provided in the supporting information Section 2. The magnetite content in the CNC@Fe_3O_4 NPs and lignin@Fe_3O_4 NPs was found to be 74.1 ± 5.1 wt% and 78.6 ± 2.1 wt%, respectively. TGA thermograms (Fig 2C) showed that lignin@Fe_3O_4 NPs possessed better thermal performance than CNC@Fe_3O_4 NPs. For example, CNC@Fe_3O_4 NPs lost about 4% of its mass below 200°C due to moisture evaporation, and at 450 ºC these lost an additional 20% mostly due to the thermal decomposition of CNC. On the other hand, lignin@Fe_3O_4 NPs only lost about 5% at 450 ºC, but went through a significant mass loss of approximately 15% between 700 and 800 °C. The high thermal stability of the lignin nanocomposite was presumably caused by the interaction with the magnetite core [11].

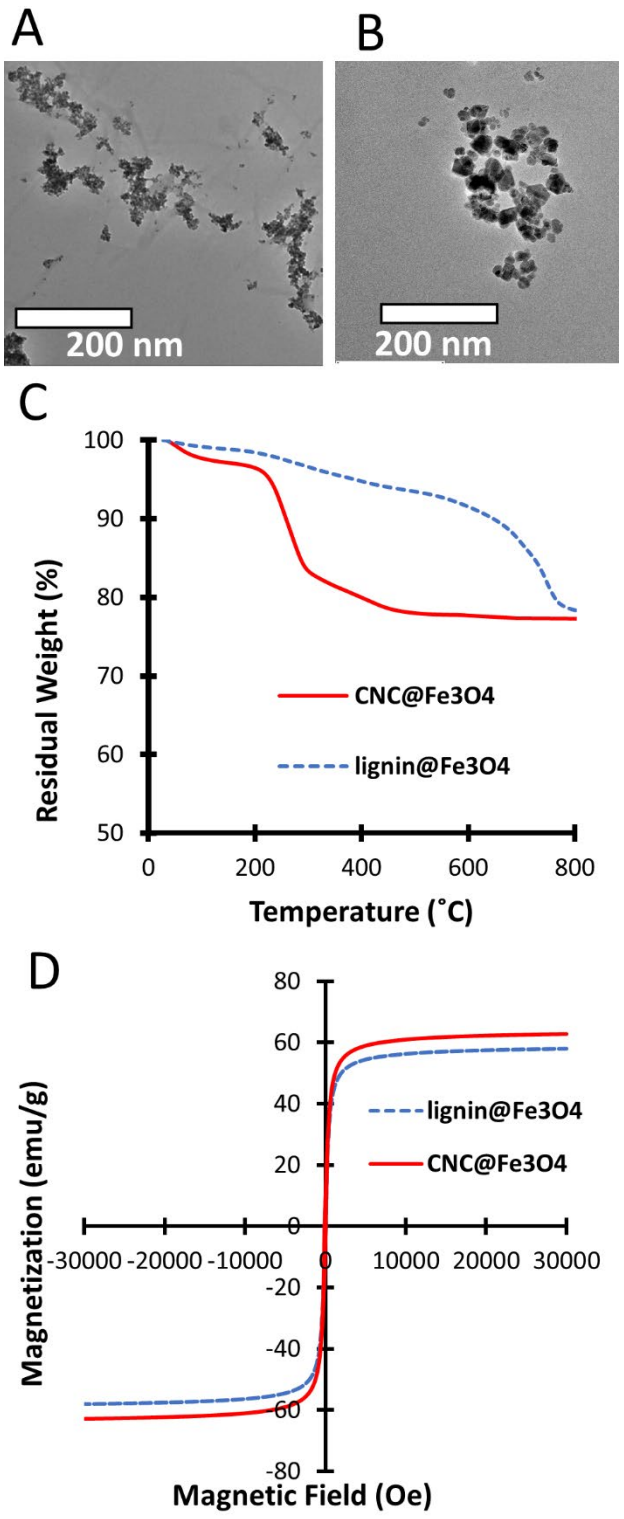

Figure 2. Characterization of CNC@Fe_3O_4 and lignin@Fe_3O_4 NPs. (A) TEM image of CNC@Fe_3O_4; (B) TEM image of lignin@Fe_3O_4; (c) TGA graph; (d) magnetization vs magnetic field.

The saturation magnetization of CNC@Fe_3O_4 and lignin@Fe_3O_4 NPs was measured in a vibrating sample magnetometer (Fig 2D). The saturation magnetization of CNC@Fe_3O_4 and lignin@Fe_3O_4 NPs was calculated to be 62 ± 1 emu/g and 58 ± 1 emu/g, respectively. When

correcting for the non-magnetic content measured by TGA, the saturation magnetization of the magnetite present in the nanocomposites is 84 ± 1 emu/gFe_3O_4 and 74 ± 1 emu/gFe_3O_4 for the CNC@Fe_3O_4 and lignin@Fe_3O_4 NPs, respectively. No hysteresis was seen in either hybrid NPs providing evidence for superparamagnetic properties of the hybrid NPs.

The size and zeta potential of the hybrid NPs was measured using a Malvern zetasizer. According to zeta potential measurements, both CNC@Fe_3O_4 and lignin@Fe_3O_4 NPs exhibited highly negative zeta potential at pH 7, i.e. -33 ± 1 mV and -40 ± 1 mV, respectively, indicating that the NPs are stable in water due to electrostatic repulsion forces between the NPs when they are dispersed in water [13]. On the other hand, bare Fe_3O_4 NPs had low zeta potential value (-20 ± 2 mV), meaning they can aggregate and precipitate over time. The hydrodynamic diameters of CNC@Fe_3O_4 and lignin@Fe_3O_4 NPs in water at pH 7 were determined to be 221 ± 5 nm and 161 ± 4 nm, respectively, whereas for bare Fe_3O_4 NPs the value was 33 ± 7 nm. The hydrodynamic diameter of bare Fe_3O_4 NPs was initially smaller than the hybrid NPs even though the zeta potential value of bare Fe_3O_4 was lower. This was when the measurements were carried out immediately following the preparation of the dispersions and probe sonication. However, the hydrodynamic diameter, measured after 2 hours, revealed that the bare Fe_3O_4 NPs aggregated significantly (1645 ± 45 nm), whereas CNC@ Fe_3O_4 and lignin@ Fe_3O_4 had hydrodynamic diameters of 321 ± 10 nm and 274 ± 9 nm, respectively, consistent to our previous publication [13]. Therefore, the presence of CNC or lignin is helpful to improve the colloidal stability of the NPs.

The water contact angle on thin films prepared with the NPs was measured using the sessile drop method. Bare Fe_3O_4 NPs are hydrophilic in nature. The water contact angle of bare Fe_3O_4 NPs film was found to be 25 ± 5 degree which is consistent to recent literature [46]. The water contact angle of CNC@Fe_3O_4 and lignin@Fe_3O_4 NPs' film was determined to be 44 ± 3 degree and 50 ± 2 degree, respectively. Therefore, combining CNC or lignin with the Fe_3O_4 NPs reduced their hydrophilicity, potentially increased their ability to stabilize the Pickering emulsions. Instability in the Pickering emulsion often results from particles that are either too hydrophilic or too hydrophobic. It has been observed that contact angles in the range of 50° to 130° occur when particle wetting by water or oil is sufficient to generate a stable Pickering emulsion [3,47–50].

3.2. *Effect of NPs on the interfacial tensions of castor oil, water, ethanol at equilibrium*

The interfacial tensions (IFT) between aqueous phases containing various concentrations (0, 0.25, 0.5, 0.75, and 1 wt%) of CNC@Fe_3O_4 and lignin@Fe_3O_4 and the corresponding organic phase in equilibrium were measured as shown in Figure 3. Our recent publication reported the liquid-liquid equilibrium of the ternary system in the presence of these NPs [12]. At the conditions tested the aqueous phase has 93.468 wt% water, 6.530 wt% ethanol and 0.002 wt% castor oil, while the organic phase has 0.470 wt% water, 1.829 wt% ethanol, and 97.701 wt% castor oil. The dynamic IFT measurements (Fig. 3B) of all samples demonstrated it decreased initially over time before reaching a plateau when the system equilibrated. The initial decrease in dynamic IFT occurs due to the migration of NPs to the interface over time. The value measured at equilibrium after 1 hour was reported as the IFT of the system in Figure 3A. Increasing the concentration of CNC@Fe_3O_4 decreased the IFT monotonically. With no added NP the IFT was 11.56 ± 0.41 mN/m; while, it dropped to 5.12 ± 0.57 mN/m when the aqueous phase had 1 wt% CNC@Fe_3O_4. Similar results were seen with the lignin@Fe_3O_4 NPs. However, the effect was lower compared to the same concentrations of CNC@Fe_3O_4, thus when the aqueous phase had 1 wt% lignin@Fe_3O_4 NPs, the IFT was 8.12 ± 0.42 mN/m. Overall, the results suggest that both CNC@Fe_3O_4 and lignin@Fe_3O_4 have a tendency to lower the energy required to create an interphase indicating their potential ability of enhancing the stability of Pickering emulsions. Moreover, CNC@Fe_3O_4 showed a greater ability of lowering IFT compared to the lignin@Fe_3O_4 NPs, suggesting the former may lead to more stable Pickering emulsions. Although, it should be noted that many other factors influence Pickering emulsions stability, such as interfacial rheology,

viscosity of the continuous phase, and nanoparticle adsorption energy. A detailed study of all parameters is outside the scope of this paper, yet a description of emulsion stability and the demulsification ability of an external magnetic field is provided in the following section.

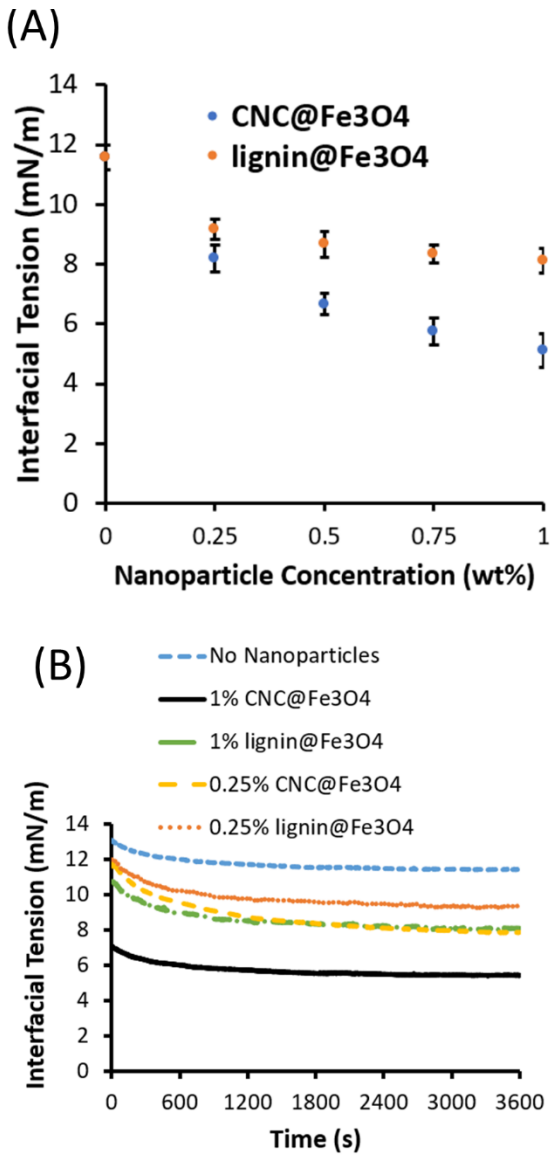

Figure 3. Interfacial tension measurements between castor oil and aqueous phases with CNC@Fe_3O_4 and lignin@Fe_3O_4. In (A) equilibrium interfacial tension, and (B) dynamic interfacial tension. Equilibrium compositions: aqueous phase (93.468 wt% water, 6.530 wt% ethanol and 0.002 wt% castor oil), organic phase (0.470 wt% water, 1.829 wt% ethanol, and 97.701 wt% castor oil).

3.3. *Pickering emulsions stability and demulsification process*

The stability of the castor oil-water-ethanol emulsion prepared without nanoparticles was investigated first as a control test with oil/aqueous-ethanol ratios of 50/50, and 70/30. The aqueous phase initially contained 10 vol% ethanol. As shown in Figure 4, significant creaming occurred in the emulsion prepared with oil to ethanol-water volume ratio of 50/50, compared to 70/30. Therefore, the emulsions prepared with 70/30 ratio had comparatively better emulsion stability, yet they started to break within a few minutes, indicating an additional stabilizer is needed. The

emulsion samples were imaged under a microscope at 0 h, and 24 hours. The average diameter of the droplets of 50/50, and 70/30 emulsions were 14.83 µm ± 10.03 µm, and 8.95 ± 6.78 µm, respectively, at time 0 h (the ± indicate one standard deviation). After 2h h, the average droplet size of 50/50 and 70/30 emulsions increased to 38.23 µm ± 22.53 µm, 11.91 µm ± 13.35 µm. The changes in droplet size was also confirmed with a hypothesis test at 95% confidence and assuming a log-normal distribution for 50/50 emulsion; however, the statistical analysis did not show enough evidence of changes in mean droplet size for 70/30 emulsion. The overall results show a statistically significant difference in the droplet size after 24 hours for the 50/50 emulsion, which is indicative of a low stability.

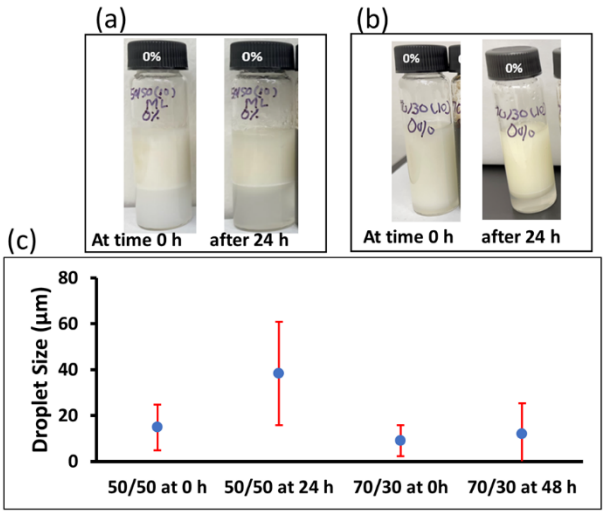

Figure 4. Control emulsions prepared at castor oil to aqueous phase volume ratio of (a) 50/50; (b) 70/30; (c) Average droplet size of the emulsions prepared at various oil/water ratios at 0 h and after 24 h. The error bars represent one standard deviation.

In this paper it is desired to prepare stable emulsions that can be readily broken by an external magnetic field. The ability to generate stable emulsions is expected to increase the interfacial area for ethanol transfer from the aqueous phase to the oil phase during a liquid/liquid extraction process. However, the quick break-up of those emulsions is required to properly decant the oil and aqueous phase after mass transfer.

The stability of the CNC@Fe_3O_4 and lignin@Fe_3O_4-stabilized Pickering emulsions was studied by visual inspection of the emulsion vials, analyzing the change in droplet size over time from the corresponding microscopy images and droplet size analysis. For the CNC@Fe_3O_4 and lignin@Fe_3O_4 -stabilized Pickering emulsions, the oil to aqueous phase ratios of 50/50, and 70/30 were used at four different NP concentrations (0.25, 0.5, 0.75 and 1 w/v%) to determine the effect of the NPs on emulsion stability (Figure 5, Figure S2, S3). The aqueous phase was made of constant 10 vol% aqueous ethanol. The pictures of 50/50 and 70/30 emulsions prepared at various concentrations of CNC@Fe_3O_4 and lignin@Fe_3O_4 are shown in figure 5 and figure S2. All emulsions were oil-in-water (O/W) type. In general, Pickering emulsions are O/W if the NPs are preferably wetted by the aqueous phase [51]. The longest-lasting emulsions were those with the highest concentrations of CNC@Fe_3O_4 and lignin@Fe_3O_4, consistent to what is observed in various nanocellulose [52] and lignin-based emulsions [11,53]. Increasing the CNC@Fe_3O_4 and lignin@Fe_3O_4 nanoparticle concentration increased the emulsion volume and decreased the creaming rate over time. The emulsions prepared with 0.75 w/v% and the 1.0 w/v% CNC@Fe_3O_4 NP concentrations showed better stability over time compared to 0.25 and 0.5 w/v%, and also successfully demulsified the oil/ethanol-water layers. Almost identical results were seen with

emulsions prepared with lignin@Fe_3O_4 NPs. In terms of oil to aqueous phase ratio, emulsions prepared with a 50/50 ratio showed higher creaming compared to 70/30 at all NPs concentrations. Hence, the 70/30 emulsions exhibited the highest stability over 24 hours. Overall, the emulsions made with a 70/30 ratio and 1 w/v% lignin@Fe_3O_4 or CNC@Fe_3O_4 NPs had the best stability of all the conditions herein investigated.

Emulsion stability was further assessed by examining the change in droplet size over a 24-hour period. It was discovered that for emulsions prepared with the 70/30 oil/aqueous phase ratio and 1.0 w/v% NP concentration, the droplet size remained almost unchanged over 24 hours. The 70/30 emulsions stabilized by 0.25 w/v%, 0.5 w/v%, and 0.75 w/v% NPs were also found to be stable for 24 hours, however, with some change in droplet size over time. Nevertheless, a statistical analysis verified that the changes in droplet size over 24 hours were not significant with a 95% confidence level across all concentrations of NPs that were examined. It should be noted, however, that a statistical analysis comparing the mean diameters of the emulsions stabilized by 1% CNC@Fe_3O_4 with those prepared with 0.25% CNC@Fe_3O_4 confirmed a larger droplet size at the lower NP concentration. -The 50/50 emulsions were not as stable as the 70/30 over time with average diameters and standard deviations increasing within that time frame. Yet, the statistical analysis did not yield enough conclusive evidence regarding variations in droplet size over a 24-hour timeframe.

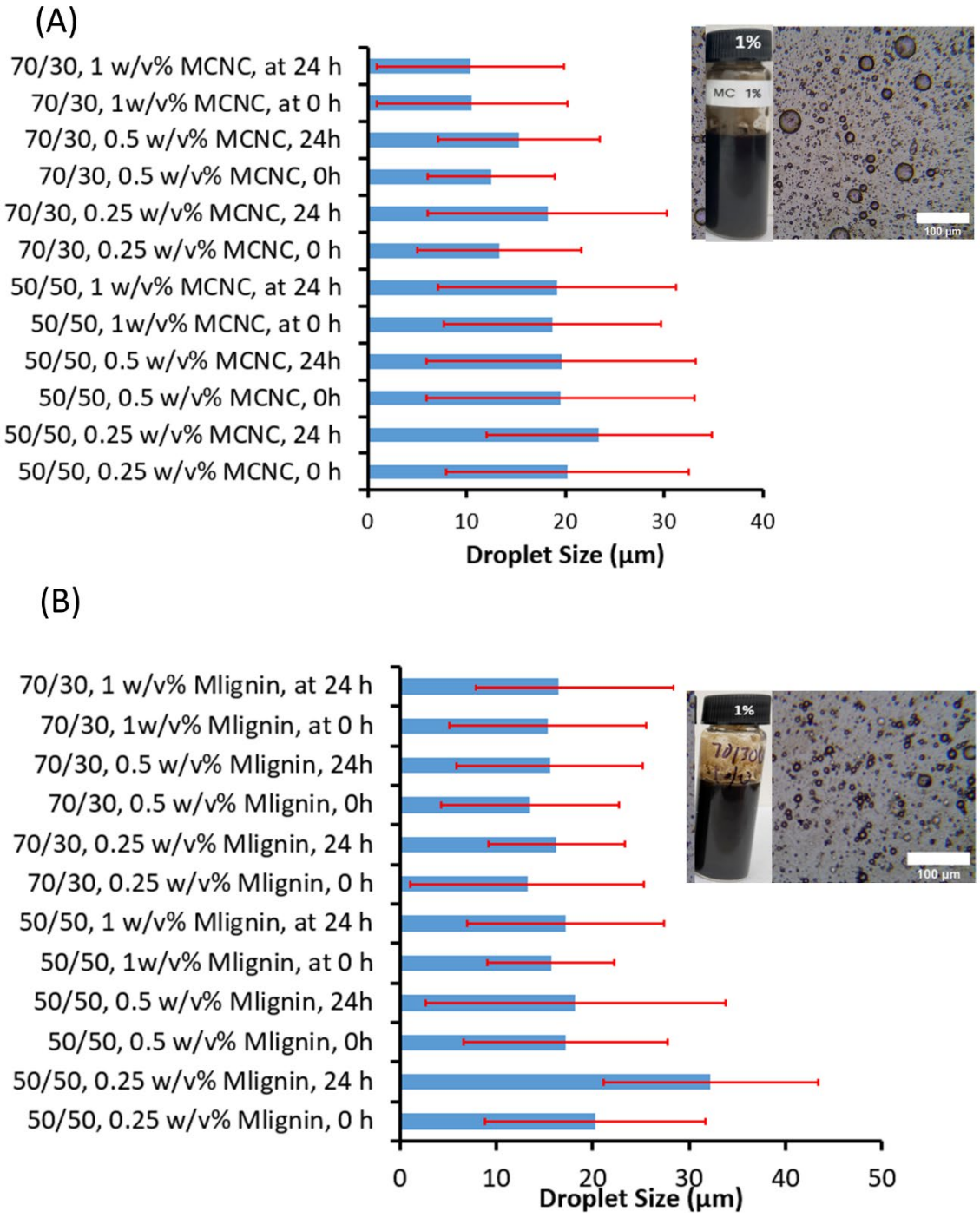

Figure 5. Droplet size distribution of the castor oil/ethanol-water Pickering emulsions stabilized with 0.25, 0.5, 0.75, and 1% NPs at oil/aqueous phase volume ratios of 50/50 and 70/30 over 24 hours. (A) emulsion stabilized with CNC@Fe_3O_4; (B) lignin@Fe_3O_4 NPs. MCNC and Mlignin indicated CNC@Fe_3O_4 and lignin@Fe_3O_4, respectively. Error bars represent one standard deviation. Insets show example microscopy picture of the 70/30 emulsions prepared with 1% NPs (Scale bar = 100 µm).

The effect of ethanol on the stability of the CNC@Fe_3O_4 and lignin@Fe_3O_4-stabilized Pickering emulsions was also studied at aqueous phase ethanol concentrations ranging from 5 vol% to 20 vol%. The corresponding pictures of 50/50 and 70/30 emulsions prepared stabilized

with a fixed 1 w/v% CNC@Fe_3O_4 and 1 w/v% lignin@Fe_3O_4 are shown in Figure 6 and Figure S4, S5. The 70/30 emulsions were found to be stable over the 24 hours period. Increasing the ethanol concentration appeared to lead to larger droplet sizes, suggesting a tendency toward coalescence and less stable emulsions. However, the changes in droplet size were not deemed statistically significant based on the analysis conducted with a 95% confidence level. Moreover, the 50/50 emulsions were also stable for all ethanol concentrations tested over time.

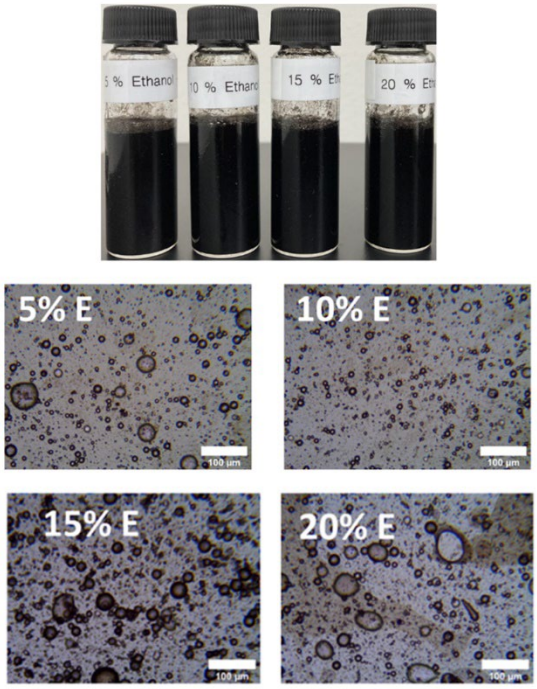

Figure 6. Castor oil/ethanol-water Pickering emulsions stabilized with 5, 10, 15 and 20% ethanol in the aqueous phase and 1 w/v% CNC@Fe_3O_4 after 24 h (Scale bar = 100 μm).

In our previous study, we successfully demulsified W/O Pickering emulsions stabilized by CNC@Fe_3O_4 NPs with a permanent magnet, however O/W emulsions remained stable after sitting for 24 h on top of the magnet [13]. In this paper, the ability of CNC@Fe_3O_4 and lignin@Fe_3O_4 NPs to demulsify the ternary {castor oil+water+ethanol} Pickering emulsions was observed by exposing them to a magnetic field of 500 mT (Figure 7, Figure S6) with all emulsions being successfully broken by the external magnetic field. In both studies the vials containing the emulsions, were placed in contact with the magnet a few minutes after emulsification, and then allowed to demulsify in the presence of the external magnetic field. When ethanol is present, it diffuses from the aqueous phase into the oil phase at the same time as the demulsification is happening. It is hypothesized that the transport of ethanol disturbs the interface, enhancing the ability of the magnet to pull the nanoparticles (NPs) out of the interface, and improving the demulsification ability of the external magnetic field. It is also possible, that the presence of ethanol has an impact on the nanoparticle adsorption energy under equilibrium conditions. As shown in Figure 3, an equilibrium system with 6.5 wt% ethanol in the aqueous phase (1.8 wt % in the oil phase) has an IFT of 11.56 ± 0.41 mN/m, while the IFT of a castor oil/water interface, without ethanol, is 14.56 ± 0.41 mN/m. The lower interfacial tension of the interface without NPs in the presence of ethanol should lower the NP adsorption energy, as shown in Parajuli et al. [3] and consequently would facilitate the removal of the NPs from the interface. Nevertheless, the effect of ethanol on the equilibrium IFT is only 3 mN/m at the conditions tested. Thus, it is

essential to note that a more extensive and comprehensive investigation is required to definitively elucidate the underlying mechanism involved in this process.

Figure 7a and 7b shows the demulsification of 50/50 emulsions, stabilized by lignin@Fe_3O_4 at varied NP and ethanol concentrations, respectively. While Figure 7c and 7d shows the demulsification of 70/30 emulsions, stabilized by lignin@Fe_3O_4 at the same NP and ethanol concentrations. Even though, all emulsions were successfully broken, increasing the NPs concentration appeared to increase the demulsification rate. During the demulsification process, the emulsion drops are pulled towards the magnet and concentrated in close proximity to it. In the high concentration region near the magnet, the drops start breaking and the magnetic NPs are removed from the interface. Very few drops remain near an interfacial region separating two bulk oil-rich and water-rich phases, but eventually most drops break up. In almost all cases, clean organic and aqueous phases remained with insignificant number of droplets left in the system. Similarly, the emulsions prepared with CNC@Fe_3O_4 at the same conditions were all successfully broken by the external magnet (Figure S6).

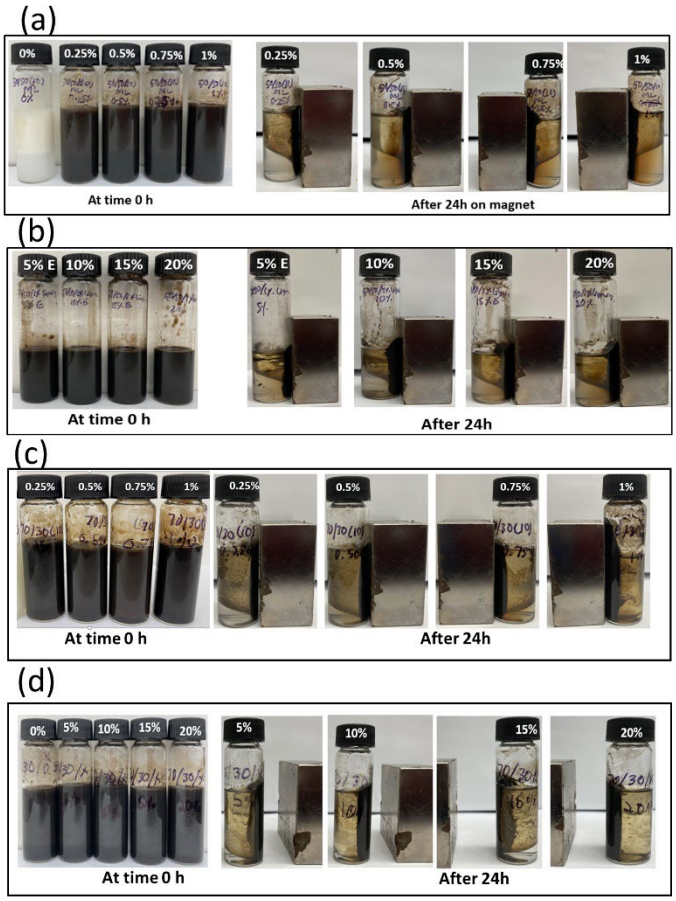

Figure 7. Demulsification experiments of emulsions stabilized by lignin@Fe_3O_4 NPs. A 50/50 oil/aqueous phase ratio is used in (a) at NP concentrations from 0.25 to 1 w/v% and (b) at ethanol concentrations of 5% to 20%. 70/30 emulsions are shown in (c) at NP concentrations from 0.25 to 1 w/v% and (d) at ethanol concentrations from 5% to 20%.

3.4. Recyclability of the magnetic NPs

The recyclability of the CNC@Fe_3O_4 and lignin@Fe_3O_4 nanoparticles on castor oil-water-ethanol Pickering emulsions was investigated over three cycles of successive emulsification and

demulsification. The nanoparticles were recovered after each demulsification and reused in the following cycle. After the third cycle the magnetic NPs were characterized with VSM and XRD and compared with the fresh NPs to investigate if they oxidized throughout the process. Figure 8a, and 8b show the recyclability of the CNC@Fe_3O_4 and lignin@Fe_3O_4 NPs, respectively, in 70/30 O/W emulsions with 10% ethanol in the aqueous phase. Results showed that the CNC@Fe_3O_4 and lignin@Fe_3O_4 NPs successfully emulsified and magnetically demulsified the emulsions at least three times. VSM results demonstrated that there is no significant decrease in saturation magnetization of the recycled nanoparticles compared to fresh NPs suggesting that the NPs retained their magnetic properties (Figure 8c). The saturation magnetization of recycled CNC@Fe_3O_4 was found to be 60 emu/g where the fresh CNC@Fe_3O_4 had 62 emu/g. Similarly, the saturation magnetization of recycled lignin@Fe_3O_4 was determined to be 56 emu/g where the fresh NPs had 58 emu/g. The saturation magnetization was calculated based on the total mass of NP used during the VSM measurements. Moreover, the XRD of the recycled NPs showed exactly the same peaks as the fresh NPs that are attributed to Fe_3O_4 nanoparticles, indicating no change in the NP crystalline morphology after their use in Pickering emulsions (Figure 8d). The XRD peaks of the fresh and recycled CNC@Fe_3O_4 and lignin@Fe_3O_4 were located at 30º, 35º, 43º, 53º, 57º, 63º, and correspond to Miller indices of (220), (311), (400), (422), (511), and (440) of a face-centered cubic lattice observed in Fe_3O_4 [31,54–56]. Thus CNC@Fe_3O_4 and lignin@Fe_3O_4 NPs can be used in the emulsification of ternary castor oil-water-ethanol emulsions and magnetically controllable demulsification for several cycles [57].

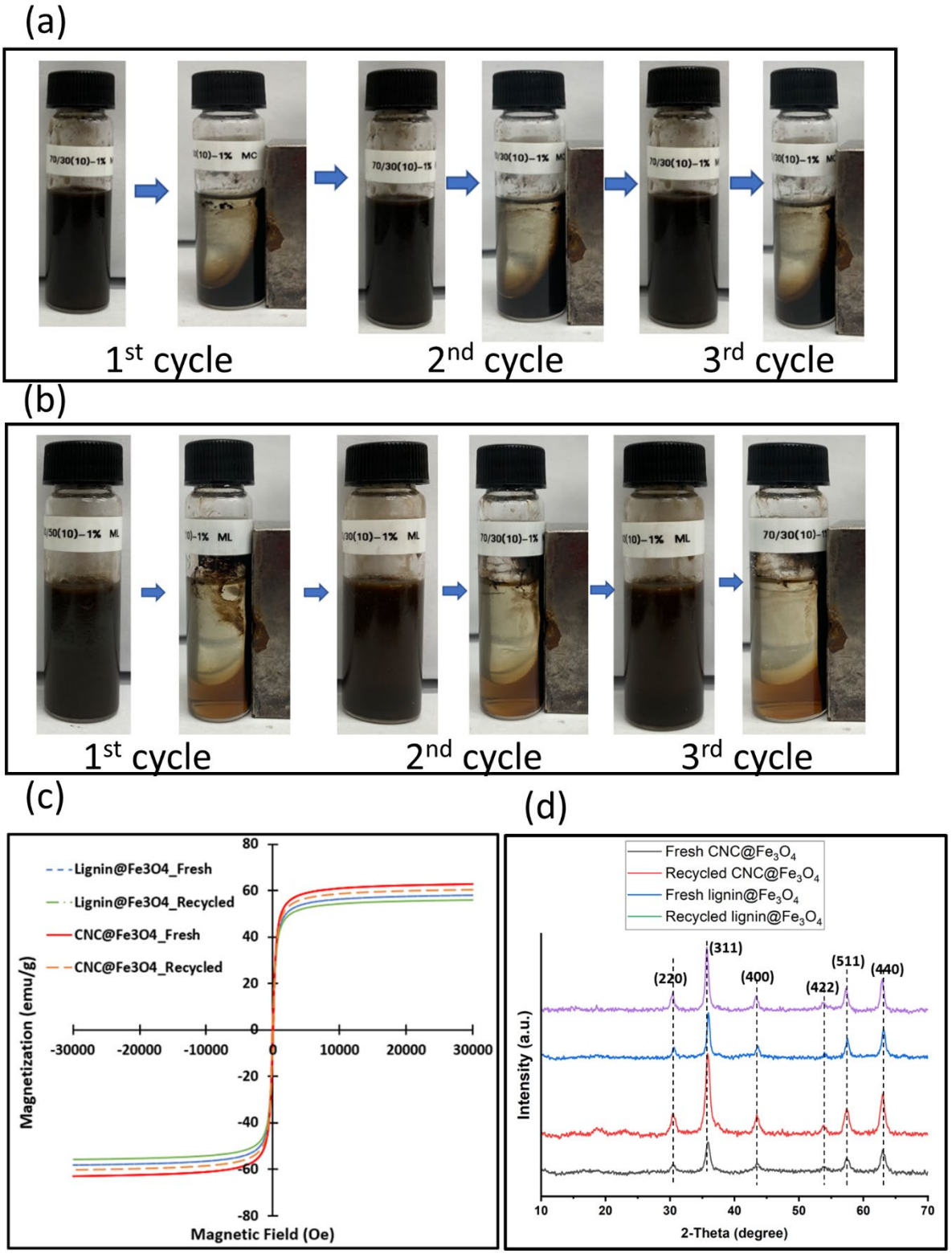

Figure 8. Recyclability of (a) CNC@Fe_3O_4; and (b) lignin@Fe_3O_4 NPs in magnetically controllable emulsification and demulsification cycles for 70/30 castor oil/aqueous phase emulsions with 10% ethanol in water. (C) VSM of fresh NPs and recycled NPs at 300 K; and (d) XRD of fresh and recycled NPs.

4. Conclusion

Castor oil/water/ethanol Pickering emulsions were prepared using CNC@Fe_3O_4 and lignin@Fe_3O_4 as a magnetically responsive emulsifying agent. These emulsions form naturally in liquid/liquid extraction systems; they accelerate mass transfer due to a larger interfacial area, yet they also slow down the separation of components after mass transfer often resulting in impractically large settling regions in industrial equipment. In the present study, all emulsions were stable in the absence of a magnetic field but were effectively broken by an external magnet. The stability of the emulsions was investigated at various castor oil to aqueous phase ratios (50/50, and 70/30), nanoparticles (NP) concentrations (0.25, 0.5, 0.75, and 1 w/v%), and ethanol concentrations in the aqueous phase (5, 10, 15, and 20%). The results showed that the emulsions prepared with a castor oil to aqueous phase volume ratios of 70/30 had higher stability with less creaming and more stable drop size distributions over 24 h, compared to the 50/50 emulsions. Increasing the NP concentration increased the emulsion stability, with 1 w/v% NPs providing the most stable emulsions, compared to 0.25, 0.5 and 0.75 w/v% NPs. The demulsification study showed that all the emulsions stabilized with CNC@Fe_3O_4 and lignin@Fe_3O_4 were successfully broken on demand by using a permanent magnet with a maximum field of 500 mT. It is interesting to note that in a previous publication, O/W emulsion stabilized by CNC@Fe_3O_4 without added ethanol could not be broken by a magnetic field [13]. Such result indicates that the presence of ethanol in this ternary system improves the ability to demulsify the system. Two plausible reasons have been proposed, which include the mass transfer of ethanol disturbing the interface, and/or a reduction in interfacial tension of the neat interface (without nanoparticles) which would lower the adsorption energy of the nanoparticles. Both reasons would facilitate the removal of a nanoparticle from the interface by a magnetic field. However, it should be noted that the effect of ethanol on interfacial tension is only 3 mN/m, which may limit the extent of its effect.

The recyclability of the NPs was demonstrated over 3 cycles. After each demulsification, the NPs were recovered and reused to prepare a new Pickering emulsion. The recycled NPs were characterized after the third cycle using XRD and VSM. The results showed that the recycled NPs retained their saturation magnetization and crystalline morphology, pointing that they can be utilized multiple times without significant degradation. Overall, this study will help develop and gain insights into three-component emulsions with magnetically controllable demulsification, with direct applications in liquid-liquid extraction, and possibly in other types of applications including magnetic separations, wastewater treatment, drug delivery, food and beverage, cosmetics and personal care, and environmental applications.

CRediT authorship contribution statement

Mohammad Jahid Hasan: Conceptualization, Investigation, Methodology, Validation, Writing – original draft. **Peng Chen:** Investigation. **Neithan Dominick:** Investigation. **Erick Vasquez:** Methodology, Writing – review & editing, Funding acquisition, Project administration. **Esteban Urena-Benavides:** Conceptualization, Writing – review & editing, Supervision, Funding acquisition, Project administration.

Declaration of Competing Interest

The authors declare that they have no known competing financial interests or personal relationships that could have appeared to influence the work reported in this paper.

Data availability

Data will be made available on request.

Acknowledgements

This work was funded in part by the National Science Foundation under Grants 1704897 and 1705331.

Appendix A. Supporting information

Supplementary data associated with this article can be found in the online version at XXXXXX.

References

[1] R.D. Offeman, S.K. Stephenson, G.H. Robertson, W.J. Orts, Solvent extraction of ethanol from aqueous solutions using biobased oils, alcohols, and esters, J. Am. Oil Chem. Soc. 83 (2006) 153–157. https://doi.org/10.1007/s11746-006-1188-9.

[2] F. Ben Cheikh, A.B. Mabrouk, A. Magnin, J.-L. Putaux, S. Boufi, Chitin nanocrystals as Pickering stabilizer for O/W emulsions: Effect of the oil chemical structure on the emulsion properties, Colloids Surf. B. 200 (2021) 111604. https://doi.org/10.1016/j.colsurfb.2021.111604.

[3] S. Parajuli, A.L. Dorris, C. Middleton, A. Rodriguez, M.O. Haver, N.I. Hammer, E. Ureña-Benavides, Surface and Interfacial Interactions in Dodecane/Brine Pickering Emulsions Stabilized by the Combination of Cellulose Nanocrystals and Emulsifiers, Langmuir. 35 (2019) 12061–12070. https://doi.org/10.1021/acs.langmuir.9b01218.

[4] S. Parajuli, O. Alazzam, M. Wang, L.C. Mota, S. Adhikari, D. Wicks, E.E. Ureña-Benavides, Surface properties of cellulose nanocrystal stabilized crude oil emulsions and their effect on petroleum biodegradation, Colloids Surf. A: Physicochem. Eng. 596 (2020) 124705. https://doi.org/10.1016/j.colsurfa.2020.124705.

[5] C. Wang, H. Jiang, Y. Li, Water-in-oil Pickering emulsions stabilized by phytosterol/chitosan complex particles, Colloids Surf. A: Physicochem. Eng. 657 (2023) 130489. https://doi.org/10.1016/j.colsurfa.2022.130489.

[6] F.-Z. Zhou, X.-H. Yu, D.-H. Luo, X.-Q. Yang, S.-W. Yin, Pickering water in oil emulsions prepared from biocompatible gliadin/ethyl cellulose complex particles, Food Hydrocoll. 134 (2023) 108050. https://doi.org/10.1016/j.foodhyd.2022.108050.

[7] F. Cui, S. Zhao, X. Guan, D.J. McClements, X. Liu, F. Liu, T. Ngai, Polysaccharide-based Pickering emulsions: Formation, stabilization and applications, Food Hydrocoll. 119 (2021) 106812. https://doi.org/10.1016/j.foodhyd.2021.106812.

[8] E. Tenorio-Garcia, A. Araiza-Calahorra, E. Simone, A. Sarkar, Recent advances in design and stability of double emulsions: Trends in Pickering stabilization, Food Hydrocoll. 128 (2022) 107601. https://doi.org/10.1016/j.foodhyd.2022.107601.

[9] S. Parajuli, M.J. Hasan, E.E. Ureña-Benavides, Effect of the Interactions between Oppositely Charged Cellulose Nanocrystals (CNCs) and Chitin Nanocrystals (ChNCs) on the Enhanced Stability of Soybean Oil-in-Water Emulsions, Mater. 15 (2022) 6673. https://doi.org/10.3390/ma15196673.

[10] S. Parajuli, E.E. Ureña-Benavides, Fundamental aspects of nanocellulose stabilized Pickering emulsions and foams, Adv. Colloid Interface Sci. 299 (2022) 102530. https://doi.org/10.1016/j.cis.2021.102530.

[11] M. Jahid Hasan, E. Westphal, P. Chen, A. Saini, I.-W. Chu, S. J. Watzman, E. Ureña-Benavides, E. S. Vasquez, Adsorptive properties and on-demand magnetic response of lignin@Fe 3 O 4 nanoparticles at castor oil–water interfaces, RSC Adv. 13 (2023) 2768–2779. https://doi.org/10.1039/D2RA07952F.

[12] M.J. Hasan, F. Yeganeh, A. Ciric, P. Chen, E.S. Vasquez, E.E. Ureña-Benavides, Liquid-liquid equilibria of water + ethanol + castor oil and the effect of cellulose nanocrystal/Fe3O4 and lignin/Fe3O4 nanoparticles, J. Chem. Thermodyn.180 (2023) 107007. https://doi.org/10.1016/j.jct.2023.107007.
[13] M.J. Hasan, F.A. Petrie, A.E. Johnson, J. Peltan, M. Gannon, R.T. Busch, S.O. Leontsev, E.S. Vasquez, E.E. Urena-Benavides, Magnetically induced demulsification of water and castor oil dispersions stabilized by Fe3O4-coated cellulose nanocrystals, Cellulose. 0123456789 (2021). https://doi.org/10.1007/s10570-021-03813-x.
[14] X. Huang, Y. Xiong, W. Yin, L. Lu, J. Liu, K. Peng, Demulsification of a New Magnetically Responsive Bacterial Demulsifier for Water-in-Oil Emulsions, Energy Fuels. 30 (2016) 5190–5197. https://doi.org/10.1021/acs.energyfuels.6b00687.
[15] H. Yang, S. Wang, W. Zhang, J. Wu, S. Yang, D. Yu, X. Wu, Y. Sun, J. Wang, Rapid demulsification of pickering emulsions triggered by controllable magnetic field, Sci. Rep. 10 (2020) 16565. https://doi.org/10.1038/s41598-020-73551-w.
[16] Y. Romanova, T. Maryutina, N. Musina, E. Yurtov, B. Spivakov, Demulsification of water-in-oil emulsions by exposure to magnetic field, J. Pet. Sci. Eng. 179 (2019). https://doi.org/10.1016/j.petrol.2019.05.002.
[17] S. Mirshahghassemi, J.R. Lead, Oil Recovery from Water under Environmentally Relevant Conditions Using Magnetic Nanoparticles, Environ. Sci. Technol. 49 (2015) 11729–11736. https://doi.org/10.1021/acs.est.5b02687.
[18] F. Zhang, Z. Yang, T. Yin, H. Shen, W. Liang, X. Li, M. Lin, J. Zhang, Z. Dong, Study of Pickering emulsions stabilized by Janus magnetic nanosheets, Colloids Surf. A: Physicochem. Eng. 654 (2022) 130194. https://doi.org/10.1016/j.colsurfa.2022.130194.
[19] I. Udoetok, L. Wilson, J. Headley, Stabilization of Pickering Emulsions by Iron oxide Nano-particles, Adv. Mater. Sci. 1 (2016). https://doi.org/10.15761/AMS.1000107.
[20] K.Y. Lin, H. Yang, C. Petit, W.D. Lee, Magnetically controllable Pickering emulsion prepared by a reduced graphene oxide-iron oxide composite, J. Colloid Interface Sci. 438 (2015) 296–305. https://doi.org/10.1016/j.jcis.2014.10.015.
[21] H. Wang, K.-Y. Lin, B. Jing, G. Krylova, G.E. Sigmon, P. McGinn, Y. Zhu, C. Na, Removal of oil droplets from contaminated water using magnetic carbon nanotubes, Water Res. 47 (2013) 4198–4205. https://doi.org/10.1016/j.watres.2013.02.056.
[22] V.I. Mikhaylov, M.A. Torlopov, I.N. Vaseneva, P.A. Sitnikov, Magnetically controlled liquid paraffin oil-in-water Pickering emulsion stabilized by magnetite/cellulose nanocrystals: Formation and Cr(VI) adsorption, Colloids Surf. A: Physicochem. Eng. 622 (2021) 126634. https://doi.org/10.1016/j.colsurfa.2021.126634.
[23] A. Pavía-Sanders, S. Zhang, J.A. Flores, J.E. Sanders, J.E. Raymond, K.L. Wooley, Robust Magnetic/Polymer Hybrid Nanoparticles Designed for Crude Oil Entrapment and Recovery in Aqueous Environments, ACS Nano. 7 (2013) 7552–7561. https://doi.org/10.1021/nn401541e.
[24] A. Kumar, G. Sharma, M. Naushad, S. Thakur, SPION/β-cyclodextrin core–shell nanostructures for oil spill remediation and organic pollutant removal from waste water, Chem. Eng. J. 280 (11) 175–187. https://doi.org/10.1016/j.cej.2015.05.126.
[25] M.J. Hasan, A.E. Johnson, E.E. Ureña-Benavides, “Greener” chemical modification of cellulose nanocrystals via oxa-Michael addition with N-Benzylmaleimide, Curr. Res. Green Sustain. Chem. 4 (2021) 100081. https://doi.org/10.1016/j.crgsc.2021.100081.
[26] L.P. Magagula, C.M. Masemola, M.A. Ballim, Z.N. Tetana, N. Moloto, E.C. Linganiso, Lignocellulosic Biomass Waste-Derived Cellulose Nanocrystals and Carbon Nanomaterials: A Review, Int. J. Mol. Sci. 23 (2022) 4310. https://doi.org/10.3390/ijms23084310.
[27] X. Xu, J. Zhou, D.H. Nagaraju, L. Jiang, V.R. Marinov, G. Lubineau, H.N. Alshareef, M. Oh, Flexible, Highly Graphitized Carbon Aerogels Based on Bacterial Cellulose/Lignin: Catalyst-Free Synthesis and its Application in Energy Storage Devices, Adv. Funct. Mater. 25 (2015) 3193–3202. https://doi.org/10.1002/adfm.201500538.
[28] C.J. Wijaya, S. Ismadji, S. Gunawan, A Review of Lignocellulosic-Derived Nanoparticles for

653 Drug Delivery Applications: Lignin Nanoparticles, Xylan Nanoparticles, and Cellulose Nanocrystals,
654 Mol. 26 (2021) 676. https://doi.org/10.3390/molecules26030676.
655 [29] I. Kalashnikova, H. Bizot, B. Cathala, I. Capron, Modulation of Cellulose Nanocrystals
656 Amphiphilic Properties to Stabilize Oil/Water Interface, Biomacromolecules. 13 (2012) 267–275.
657 https://doi.org/10.1021/bm201599j.
658 [30] L. Dai, Y. Li, F. Kong, K. Liu, C. Si, Y. Ni, Lignin-Based Nanoparticles Stabilized Pickering
659 Emulsion for Stability Improvement and Thermal-Controlled Release of trans-Resveratrol, ACS Sustain.
660 Chem. Eng. 7 (2019) 13497–13504. https://doi.org/10.1021/acssuschemeng.9b02966.
661 [31] F.A. Petrie, J.M. Gorham, R.T. Busch, S.O. Leontsev, E.E. Ureña-Benavides, E.S. Vasquez,
662 Facile fabrication and characterization of kraft lignin@Fe3O4 nanocomposites using pH driven
663 precipitation: Effects on increasing lignin content, Int. J. Biol. Macromol. 181 (2021) 313–321.
664 https://doi.org/10.1016/j.ijbiomac.2021.03.105.
665 [32] L. Bai, S. Lv, W. Xiang, S. Huan, D.J. McClements, O.J. Rojas, Oil-in-water Pickering emulsions
666 via microfluidization with cellulose nanocrystals: 1. Formation and stability, Food Hydrocoll.. 96 (2019)
667 699–708. https://doi.org/10.1016/j.foodhyd.2019.04.038.
668 [33] Y. Wang, X. Li, C. Shen, Z. Mao, H. Xu, Y. Zhong, X. Sui, X. Feng, B. Wang, Lignin assisted
669 Pickering emulsion polymerization to microencapsulate 1-tetradecanol for thermal management, Int. J.
670 Biol. Macromol. 146 (2020) 1–8. https://doi.org/10.1016/j.ijbiomac.2019.12.175.
671 [34] L.E. Low, L.T.-H. Tan, B.-H. Goh, B.T. Tey, B.H. Ong, S.Y. Tang, Magnetic cellulose
672 nanocrystal stabilized Pickering emulsions for enhanced bioactive release and human colon cancer
673 therapy, Int. J. Biol. Macromol. 127 (2019) 76–84. https://doi.org/10.1016/j.ijbiomac.2019.01.037.
674 [35] L.E. Low, B.T. Tey, B.H. Ong, E.S. Chan, S.Y. Tang, Palm olein-in-water Pickering emulsion
675 stabilized by Fe3O4-cellulose nanocrystal nanocomposites and their responses to pH, Carbohyd. Polym.
676 155 (2017) 391–399. https://doi.org/10.1016/j.carbpol.2016.08.091.
677 [36] T. Nypelö, C. Rodriguez-Abreu, J. Rivas, M.D. Dickey, O.J. Rojas, Magneto-responsive hybrid
678 materials based on cellulose nanocrystals, Cellulose. 21 (2014) 2557–2566.
679 https://doi.org/10.1007/s10570-014-0307-2.
680 [37] E.G.O. Grance, F.G. Souza, A. Varela, E.D. Pereira, G.E. Oliveira, C.H.M. Rodrigues, New
681 petroleum absorbers based on lignin-CNSL-formol magnetic nanocomposites, J. Appl. Polym. Sci. 126
682 (2012) E305–E312. https://doi.org/10.1002/app.36998.
683 [38] K.A. Mahmoud, M. Zourob, Fe3O4/Au nanoparticles/lignin modified microspheres as effectual
684 surface enhanced Raman scattering (SERS) substrates for highly selective and sensitive detection of
685 2,4,6-trinitrotoluene (TNT), Analyst. 138 (2013) 2712–2719. https://doi.org/10.1039/C3AN00261F.
686 [39] Y. Li, M. Wu, B. Wang, Y. Wu, M. Ma, X. Zhang, Synthesis of Magnetic Lignin-Based Hollow
687 Microspheres: A Highly Adsorptive and Reusable Adsorbent Derived from Renewable Resources, ACS
688 Sustain. Chem. Eng. (2016). https://doi.org/10.1021/acssuschemeng.6b01244.
689 [40] D. Kołodyńska, M. Gęca, I.V. Pylypchuk, Z. Hubicki, Development of New Effective Sorbents
690 Based on Nanomagnetite, Nanoscale Res. Lett. 11 (2016) 152. https://doi.org/10.1186/s11671-016-1371-
691 3.
692 [41] T. Zhang, A. Davidson, S.L. Bryant, C. Huh, Nanoparticle-Stabilized Emulsions for Applications
693 in Enhanced Oil Recovery, in: OnePetro, 2010. https://doi.org/10.2118/129885-MS.
694 [42] X. Xie, Y. Wang, X. Li, X. Wei, S. Yang, Pickering emulsions stabilized by amphiphilic
695 carbonaceous materials derived from wheat straw, Colloids Surf. A: Physicochem. Eng. 558 (2018) 65–
696 72. https://doi.org/10.1016/j.colsurfa.2018.08.063.
697 [43] G. Liu, W. Li, X. Qin, Q. Zhong, Pickering emulsions stabilized by amphiphilic anisotropic
698 nanofibrils of glycated whey proteins, Food Hydrocoll. 101 (2020) 105503.
699 https://doi.org/10.1016/j.foodhyd.2019.105503.
700 [44] X. Qiao, J. Zhou, B.P. Binks, X. Gong, K. Sun, Magnetorheological behavior of Pickering
701 emulsions stabilized by surface-modified Fe3O4 nanoparticles, Colloids Surf. A: Physicochem. Eng. 412
702 (2012) 20–28. https://doi.org/10.1016/j.colsurfa.2012.06.026.
703 [45] Jiang, L., M. Rekkas, and A. Wong. Comparing the means of two log-normal distributions: A

likelihood approach. J. Stat. Economet. Meth. 3, no. 1 (2014) 137-152.
[46] T. Lü, D. Qi, D. Zhang, Y. Lü, H. Zhao, A facile method for emulsified oil-water separation by using polyethylenimine-coated magnetic nanoparticles, J Nanopart Res. 20 (2018). https://doi.org/10.1007/s11051-018-4193-7.
[47] T. Nallamilli, M.G. Basavaraj, Synergistic stabilization of Pickering emulsions by in situ modification of kaolinite with non ionic surfactant, Appl. Clay Sci. 148 (2017) 68–76. https://doi.org/10.1016/j.clay.2017.07.038.
[48] J. Wang, F. Yang, J. Tan, G. Liu, J. Xu, D. Sun, Pickering Emulsions Stabilized by a Lipophilic Surfactant and Hydrophilic Platelike Particles, Langmuir. 26 (2010) 5397–5404. https://doi.org/10.1021/la903817b.
[49] I. Akartuna, A.R. Studart, E. Tervoort, U.T. Gonzenbach, L.J. Gauckler, Stabilization of Oil-in-Water Emulsions by Colloidal Particles Modified with Short Amphiphiles, Langmuir. 24 (2008) 7161–7168. https://doi.org/10.1021/la800478g.
[50] R. Aveyard, B.P. Binks, J.H. Clint, Emulsions stabilised solely by colloidal particles, Adv. Colloid Interface Sci. 100–102 (2003) 503–546. https://doi.org/10.1016/S0001-8686(02)00069-6.
[51] I. A. Udoetok, L.D. Wilson, J. V. Headley, Stabilization of Pickering Emulsions by Iron oxide Nano-particles (Fe3O4 NPs), Adv. Mater. Sci. 1 (2016) 24–33. https://doi.org/10.15761/ams.1000107.
[52] C. Jiménez Saelices, I. Capron, Design of Pickering Micro- and Nanoemulsions Based on the Structural Characteristics of Nanocelluloses, Biomacromolecules. 19 (2018) 460–469. https://doi.org/10.1021/acs.biomac.7b01564.
[53] S. Guo, X. Li, Y. Kuang, J. Liao, K. Liu, J. Li, L. Mo, S. He, W. Zhu, J. Song, T. Song, O.J. Rojas, Residual lignin in cellulose nanofibrils enhances the interfacial stabilization of Pickering emulsions, Carbohydr. Polym. 253 (2021) 117223. https://doi.org/10.1016/j.carbpol.2020.117223.
[54] F. Petrie, Magnetic-Lignin Nanoparticles as Potential Ethanol Extractants From Aqueous Solutions, University of Dayton, 2019.
[55] T.-J. Yoon, H. Lee, H. Shao, S. Hilderbrand, R. Weissleder, Multicore Assemblies Potentiate Magnetic Properties of Biomagnetic Nanoparticles, Adv. Mater. 23 (2011) 4793–4797.
[56] M. Ounacer, A. Essoumhi, M. Sajieddine, A. Razouk, B.F.O. Costa, S.M. Dubiel, M. Sahlaoui, Structural and Magnetic Studies of Annealed Iron Oxide Nanoparticles, J. Supercond. Nov. Magn. 33 (2020) 3249–3261. https://doi.org/10.1007/s10948-020-05586-z.
[57] M. J. Hasan, Surface Modifications of Cellulose Nanocrystals: Applications in Stabilization and Demulsification of Magnetically Controlled Castor Oil/Water/Ethanol Pickering Emulsions for Liquid-Liquid Extraction of Ethanol from Water, The University of Texas at San Antonio, ProQuest Dissertations Publishing, 2022. https://www.proquest.com/docview/2702488214/6C32E679EF0B4882PQ/1?accountid=7122